Distributed Base Station Cooperation with Finite Alphabet and QoS Constraints

Min Li and Chunshan Liu and Stephen V. Hanly
Department of Engineering, Macquarie University, Sydney, NSW 2109, Australia
Email: {min.li, chunshan.liu, stephen.hanly}@mq.edu.au

***Abstract*—This work studies a novel power-efficient precoder design problem for a linear cellular array with base station (BS) cooperation: data symbols intended for mobile stations (MSs) are drawn from discrete finite alphabets, precoding is performed among BSs to produce appropriate signals transmitted over the channel, symbol-by-symbol detection is performed at each MS, and a minimum Symbol Error Probability (SEP) for detection is introduced as the Quality-of-Service (QoS) metric at each MS. With regular constellations such as 16-QAM deployed as system data inputs, the SEP constraints are formulated and characterized by a set of convex relaxations on the received signals. A convex power optimization problem is then formulated subject to the SEP constraints. By the primal-dual decomposition approach, a distributed algorithm is developed to solve the problem in which only local communication among BSs is required. Our scheme is shown to significantly outperform linear zero-forcing precoder in terms of transmit power consumption.**

I. Introduction

Base station (BS) cooperation is considered as one of the promising approaches to cope with inter-cell interference and to increase capacity of the cellular network [1]. When all BSs share their messages and channel knowledge perfectly with a central unit, the network downlink is converted into a virtual multi-input multi-output (MIMO) broadcast channel. Then the optimal dirty-paper coding scheme or any suboptimal beamforming strategies such as zero-forcing (ZF) beamforming [2] can be applied at the central unit. In principle, remarkable system performance improvement can be accrued from the centralized BS cooperation. However, building such a central unit may be expensive and if it fails, the whole network fails. A distributed network where BSs are connected and cooperate locally may be advantageous from this point of view.

Existing research outcomes on the network with local BS cooperation can be found in [1] and the references therein. In this work, we contribute to this theme by studying the optimal cooperation strategy when total power consumption across BSs and Quality of Service (QoS) requirements at mobile stations (MSs) are primary concerns. Specifically, we consider a downlink network with local BS cooperation as shown in Fig. 1: all BSs and MSs are situated along a linear array; any two adjacent BSs are connected via bidirectional backhaul links so that they can communicate with each other and cooperate on transmission of data symbols to their intended MSs; each MS only connects to the BS in its own cell and the BSs in its nearest neighboring cells. This model is referred to as a linear cellular array with local BS cooperation.

Under the assumption that the data symbols transmitted by BSs are selected from discrete finite alphabets, such as constellations of quadrature amplitude modulation (QAM), we take a symbol detection point of view and impose minimum Symbol Error Probability (SEP) as QoS constraints at MSs. With focus on the system with 16-QAM as inputs, we first define the SEP constraints and approximate them by a set of convex relaxations on the received signals. We then formulate a power-efficient precoding optimization problem with SEP requirements at MSs and show that the resulting problem is convex. To enable local BS cooperation, we leverage the primal-dual decomposition approach and develop a distributed algorithm to solve the problem which only requires local information exchanging between neighboring BSs. A relaxation approach was also proposed in [3] for the centralized MIMO system with focus on binary and 4-QAM signaling. A difference here is that in our formulation we relax about the *received signals*, not the input data symbols, which allows us to naturally integrate the SEP targets into a convex optimization problem. In addition, our primal-dual algorithm allows distributed implementation in a network MIMO system [1].

The remainder of this paper is organized as follows. Section II formalizes the system model and Section III presents the general problem formulation. The distributed algorithm proposed is then detailed in Section IV. Numerical results are provided in Section V. Conclusions are drawn in Section VI.

Notations: Capital and lower-case bold fonts denote matrices and vectors, respectively, e.g., $\mathbf{A}$ is a matrix and $\mathbf{a}$ is a vector; notation $(\cdot)^T$ denotes the matrix transpose, while notation $(\cdot)^H$ denotes the Hermitian transpose; $\Re\{\cdot\}$ and $\Im\{\cdot\}$ are the real and imaginary parts of a complex value, respectively;$\|\mathbf{A}\|_p$ denote the standard l_p norm of matrix $\mathbf{A}$. Finally, $\sqrt{-1} = \mathrm{j}$.

II. System model

We focus on the downlink communication of a linear cellular array as illustrated in Fig. 1. In the system, we assume that the number of BSs is M and equals to the number of active MSs. Let $\mathbf{d} = [d_1, ..., d_M]$ be a set of data symbols, with each d_m selected from a set of finite alphabet $\mathcal{S}_m$ and denoting the symbol intended for MS m. At each time instant, the vector $\mathbf{d}$ is encoded and transmitted from BSs to MSs. Let x_m denote the transmit signal from BS m. Mathematically, the system

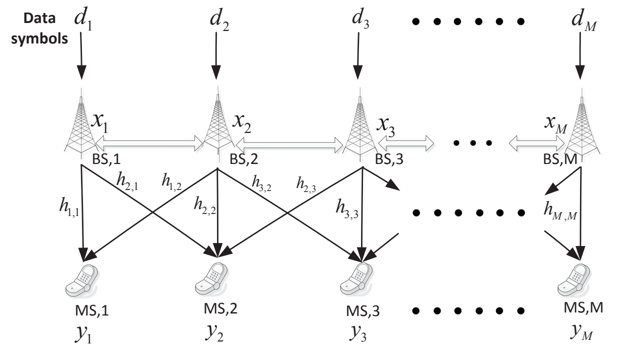

Fig. 1. A linear cellular array model with local BS cooperation on transmission of finite-alphabet symbols, and with SEP as QoS target at each MS.

model is represented as

$$y_m = \sum\nolimits_{k \in \mathbf{I}(m)} h_{m,k} x_k + v_m, m = 1, \ldots, M, \tag{1}$$

where y_m is the received signal at MS m, $\mathbf{I}(m)$ is a set of indices of the adjacent cells of cell m, $h_{m,k}$ denotes the complex channel coefficient from the kth BS to the mth MS, and v_ms are mutually independent, circularly-symmetric complex Gaussian noises all with zero mean and variance $2\sigma^2$. Alternatively the system can be represented as

$$\mathbf{y} = \mathbf{H}\mathbf{x} + \mathbf{v}, \tag{2}$$

where we have defined $\mathbf{x} \in \mathbb{C}^{M \times 1}$ as the transmitted signal vector, $\mathbf{v}$ as the noise vector, and channel matrix $\mathbf{H} = [\mathbf{h}_1, \ldots, \mathbf{h}_M]^T \in \mathbb{C}^{M \times M}$ with each component $h_{m,k}$ of $\mathbf{h}_m$ denoting the channel from the kth BS to the mth MS. Due to the locality of the inter-cell interference in the system, it is noted that channel matrix $\mathbf{H}$ is a tridiagonal matrix with band three. This particular structure is the crucial property that we can leverage to develop the distributed algorithm later.

III. Problem formulation

For the system considered, we wish to construct an efficient mapping (precoding) from the symbol-vector $\mathbf{d}$ to the transmit signal-vector $\mathbf{x}$ such that the total power consumption across the network is minimised and the set of SEP targets at MSs are satisfied. To this end, we first characterize the set of constraints prescribed by the SEP targets. Specifically, a SEP requirement indicates that the signal y_m received at MS m should potentially reside in the right decision region associated with d_m. In other words, the probability of y_m lying outside the region should be no greater than the target, i.e.,

$$\Pr(y_m = (\mathbf{h}_m^T \mathbf{x} + v_m) \notin \mathcal{A}(d_m)) \le Pe_m, \tag{3}$$

where $d_m \in \mathcal{S}_m$, $\mathcal{A}(d_m)$ corresponds to the decision region of symbol d_m, and Pe_m is the SEP target at MS m. Then the power-efficient precoding optimization problem is defined as:

$$\mathcal{P}: \begin{cases} \min\limits_{\mathbf{x}} P(\mathbf{x}) = \mathbf{x}^H \mathbf{x} \\ \text{subject to } \Pr((\mathbf{h}_m^T \mathbf{x} + v_m) \notin \mathcal{A}(d_m)) \le Pe_m, \\ \text{for a fixed set of } \{d_m \in \mathcal{S}_m, m = 1, \ldots, M\}. \end{cases} \tag{4}$$

In the following, we elaborate on how to capture the SEP constraints in (4) in a tractable manner, with focus on systems with 16-QAM constellation. Similar approach can be applied to systems with 4-QAM or higher-order QAM constellations.

A. Characterizing SEP Constraints for 16-QAM

Consider the gray-coded 16-QAM constellation as shown in Fig. 2. With a fixed noise variance, due to the SEP requirement at MS m, the constellation set $\mathcal{S}_m = \{s_j : j = 1, \ldots, 16\}$ is a scaled version of the standard one (whose inner points are the four corner-points of a unit-square) by β_m. The green dashed lines partition the complex plane into squared-shape decision regions centered on the constellation points $\{s_j\}$; any received signals falling into the decision region centred on s_j are mapped back onto s_j. Requirement (3) ensures the probability of the received signal lying outside the right decision region should be no greater than Pe_m and thus imposes a set of constraints on the received signals. Define $\overline{y}_m^{(r)} = \Re\{\mathbf{h}_m^T \mathbf{x}\}$, $\overline{y}_m^{(i)} = \Im\{\mathbf{h}_m^T \mathbf{x}\}$, $v_m^{(r)} = \Re\{v_m\}$, $v_m^{(i)} = \Im\{v_m\}$, $d_m^{(r)} = \Re\{d_m\}$ and $d_m^{(i)} = \Im\{d_m\}$. Then requirement (3) is equivalent to

$$\underbrace{\frac{1}{\sqrt{2\pi}\sigma} \int_{d_m^{(r)} - \overline{y}_m^{(r)} - \rho_-^{(r)}}^{d_m^{(r)} - \overline{y}_m^{(r)} + \rho_+^{(r)}} e^{-\frac{\left(v_m^{(r)}\right)^2}{2\sigma^2}} dv_m^{(r)}}_{\mathcal{O}^{(r)}} \bullet$$

$$\underbrace{\frac{1}{\sqrt{2\pi}\sigma} \int_{d_m^{(i)} - \overline{y}_m^{(i)} - \rho_-^{(i)}}^{d_m^{(i)} - \overline{y}_m^{(i)} + \rho_+^{(i)}} e^{-\frac{\left(v_m^{(i)}\right)^2}{2\sigma^2}} dv_m^{(i)}}_{\mathcal{O}^{(i)}} \ge 1 - Pe_m, \tag{5}$$

where $\rho_+^{(r)}/\rho_+^{(i)}$ and $\rho_-^{(r)}/\rho_-^{(i)}$ relate to the decision regions and parameterize the upper and lower bounds for the integrals. Table I specifies these parameters for 16-QAM constellations.

Given a target Pe_m, one can determine the constraint region on $\mathbf{h}_m^T \mathbf{x}$ from inequality (5). In particular, the boundary of the region may be determined by the equality $\mathcal{O}^{(r)} \mathcal{O}^{(i)} = 1 - Pe_m$ in (5). Since different constellation points are associated with different decision regions, the resulting constraints are different. Taking the side point s_{12} as an example, we point out that a set of critical points on the boundary of the constraint region can be identified by considering combinations of $(\mathcal{O}^{(r)}, \mathcal{O}^{(i)})$:

- $(\frac{1-Pe_m}{\eta}, \eta)$: $\overline{y}_m^{(r)} = 2\beta_m - \sigma Q^{-1}\left(\frac{1-Pe_m}{\eta}\right)$, $\overline{y}_m^{(i)} = \beta_m$;
- $(\sqrt{1-Pe_m}, \sqrt{1-Pe_m})$: $\overline{y}_m^{(r)} = 2\beta_m - \sigma Q^{-1}(\sqrt{1-Pe_m})$, $\overline{y}_m^{(i)} = \beta_m \pm \delta_0$;
- $(1, 1-Pe_m)$: $\overline{y}_m^{(r)} = +\infty$, $\overline{y}_m^{(i)} = \beta_m \pm \delta_1$,

where $Q^{-1}(\cdot)$ is the inverse of the standard Q-function, $\eta = \frac{1}{\sqrt{2\pi}\sigma} \int_{-\beta_m}^{\beta_m} e^{-\frac{v^2}{2\sigma^2}} dv$ and parameter δ_0 and δ_1 are chosen according to:

$$\begin{cases} Q\left(\frac{\delta_0 - \beta_m}{\sigma}\right) - Q\left(\frac{\delta_0 + \beta_m}{\sigma}\right) = \sqrt{1 - Pe_m}, \\ Q\left(\frac{\delta_1 - \beta_m}{\sigma}\right) - Q\left(\frac{\delta_1 + \beta_m}{\sigma}\right) = 1 - Pe_m. \end{cases} \tag{6}$$

In principle, the curved-shape boundary of the constraint regions can be determined by traversing all possible combinations of $\mathcal{O}^{(r)}$ and $\mathcal{O}^{(i)}$. However, there is an infinite

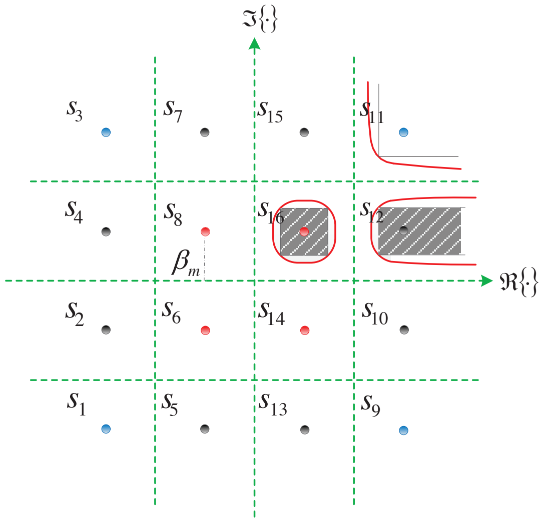

Fig. 2. 16 QAM: β_m is a scaling factor; $s_1, s_2, \ldots, s_{16}$ are constellation points; decision regions are separated by green dashed lines; linear constraints on $\mathbf{h}_m^T\mathbf{x}$ are marked by shadow areas.

number of combinations. A practical approach is to find a polytype contained in the constraint region, i.e., we conservatively approximate the region using the area bounded by line segments between a finite number of points on or within boundary. A simple approximation is exemplified with points $\{s_{11}, s_{12}, s_{16}\}$:

- s_{11}: $\overline{y}_m^{(r)} \geq 2\beta_m - \sigma Q^{-1}(\sqrt{1-Pe_m})$ and $\overline{y}_m^{(i)} \geq 2\beta_m - \sigma Q^{-1}(\sqrt{1-Pe_m})$;
- s_{12}: $\overline{y}_m^{(r)} \geq 2\beta_m - \sigma Q^{-1}(\sqrt{1-Pe_m})$ and $\beta_m - \delta_0 \leq \overline{y}_m^{(i)} \leq \beta_m + \delta_0$;
- s_{16}: $\beta_m - \delta_0 \leq \overline{y}_m^{(r)} \leq \beta_m + \delta_0$ and $\beta_m - \delta_0 \leq \overline{y}_m^{(i)} \leq \beta_m + \delta_0$,

which lead to linear constraints on $\mathbf{h}_m^T\mathbf{x}$. The regions constructed are illustrated in Fig. 2 (shadow areas) along with the true regions obtained numerically (red-curve regions).

B. Discussion on Choice of Scaling Factor β_m

In the formulation, given a noise variance, there exists a minimum requirement on the scaling factor $\beta_m \geq \beta_m^-$ such that each SEP target can be satisfied. This minimum β_m^- can be found by considering only the four center constellation points, i.e., $\{s_6, s_8, s_{14}, s_{16}\}$, as for these four points, the integral limits in (5) are more restricted than others, yielding the worst case among all constellations. Specifically, by noticing that the length of integral intervals for both the real and imaginary part is equal to $2\beta_m$ and that the noise is zero-mean, we have the following:

$$\left(\frac{1}{\sqrt{2\pi}\sigma}\int_{-\beta_m}^{\beta_m} e^{-\frac{v^2}{2\sigma^2}}dv\right)^2 \geq \mathcal{O}^{(r)}\mathcal{O}^{(i)} \geq 1 - Pe_m. \quad (7)$$

The minimum β_m^- then corresponds to the solution of (7) when equality holds and can be calculated by

$$\beta_m^- = \sigma Q^{-1}\left(\frac{1}{2} - \frac{1}{2}\sqrt{1-Pe_m}\right). \quad (8)$$

TABLE I
INTEGRAL PARAMETERS ASSOCIATED WITH THE 16-QAM CONSIDERED

$\rho_-^{(r)}/\rho_+^{(r)}$ \ $\rho_-^{(i)}/\rho_+^{(i)}$	$+\infty/\beta_m$	β_m/β_m	$\beta_m/+\infty$
$+\infty/\beta_m$	s_1	s_2, s_4	s_3
β_m/β_m	s_5, s_{13}	s_6, s_8, s_{14}, s_{16}	s_7, s_{15}
$\beta_m/+\infty$	s_9	s_{10}, s_{12}	s_{11}

It is remarked that such a minimum scaling factor imposes the most extreme constraint on the received signal when one of the four centre constellation points is transmitted:

$$\mathbf{h}_m^T\mathbf{x} = s_j, \quad j \in \{6, 8, 14, 16\}. \quad (9)$$

Therefore, we are doing a full ZF on both the real and imaginary parts of the signals when center points are transmitted. While with the same β_m^-, the constraints of the side points, e.g., s_{12}, become: $\overline{y}_m^{(r)} \geq 2\beta_m^- - \sigma Q^{-1}(\sqrt{1-Pe_m})$ and $\overline{y}_m^{(i)} = \beta_m^-$. This is equivalent to doing a ZF for the imaginary part while having a relaxed constraint on the real part of the received signal. The relaxation naturally admits a more flexible choice of coded signals and hence brings advantage.

Choosing a larger scaling factor β_m above β_m^- may or may not improve the performance. Fig. 3 plots two instances of the constraint regions when the constellation is scaled up with $\beta_m = 1.05\beta_m^-$ (blue curves) and $\beta_m = 1.20\beta_m^-$ (red curves). It can be seen that with a larger β_m above β_m^-, the constraints are relaxed for the center points. In particular, the corresponding constraint region on $\mathbf{h}_m^T\mathbf{x}$ gets enlarged and subsumes the region with smaller β_m, hence potential benefit can be accrued. However, the constraint regions for the corner points always shrink as the constellation is scaled up. In this case, potential power efficiency loss may be induced because the choice of $\mathbf{h}_m^T\mathbf{x}$ becomes more restricted. When one of the side points is transmitted, it is unclear how the performance reacts as the constraint regions with larger β_m partially overlaps with that for a smaller β_m. In general, we have observed from our extensive experiments that scaling up the constellation cannot bring significant power reduction. Therefore, fixing the scaling factor at the minimum value is reasonable as it will not incur much loss in optimality.

IV. DISTRIBUTED ALGORITHM

As seen in the previous section, the SEP constraints can be approximated by a set of linear equalities/inequalities on $\mathbf{x}$. In the following, we first present the resulting problem and then propose a distributed algorithm to solve it.

For ease of exposition, we stack the real and the imaginary parts of each x_m into a real vector $\tilde{\mathbf{x}}$, i.e., $\tilde{\mathbf{x}} = [\Re\{x_1\}, \Im\{x_1\}, \ldots, \Re\{x_M\}, \Im\{x_M\}]^T \in \mathbb{R}^{2M\times 1}$. Note that when $\beta_m = \beta_m^-$, one equality (or inequality) may be imposed on either the real or the imaginary part of the coded signal at each BS; when $\beta_m > \beta_m^-$, at most two inequalities are introduced for either the real or the imaginary part. Then the

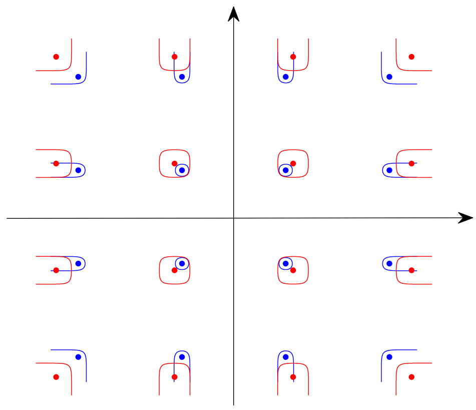

Fig. 3. Constraint regions on $\mathbf{h}_m^T\mathbf{x}$ with different scaling factors at $Pe_m = 10^{-3}$: (1) Blue curves: $\beta_m = 1.05\beta_m^-$; (2) Red curves: $\beta_m = 1.20\beta_m^-$.

optimization problem of (4) can be represented as follows:

$$\mathcal{P}_1 : \begin{cases} \min\limits_{\tilde{\mathbf{x}}\in\mathbb{R}^{2M\times 1}} P(\tilde{\mathbf{x}}) = \tilde{\mathbf{x}}^T\tilde{\mathbf{x}} \\ \text{s. t.} \quad \mathbf{U}\tilde{\mathbf{x}} - \mathbf{b} \preceq \mathbf{0}, \\ \qquad \mathbf{A}\tilde{\mathbf{x}} - \mathbf{c} = \mathbf{0}, \end{cases} \tag{10}$$

where we have matrices $\mathbf{U} = \{u_{i,j}\} \in \mathbb{R}^{4M\times 2M}$ and $\mathbf{A} = \{a_{i,j}\} \in \mathbb{R}^{2M\times 2M}$, whose precise definitions generally depend on the channel matrix and the data symbols to be transmitted; and vectors $\mathbf{b} = [b_1, \ldots, b_{4M}]^T \in \mathbb{R}^{4M\times 1}$, $\mathbf{c} = [c_1, \ldots, c_{2M}]^T \in \mathbb{R}^{2M\times 1}$, whose precise definitions depend on the data symbols, the scaling factor as well as the SEP targets. Given a set of transmitted symbols, some of the inequality/equality constraints may not be active, so the corresponding row entries of $\mathbf{U}/\mathbf{A}$ and $\mathbf{b}/\mathbf{c}$ are padded with zeros. It is further remarked that when indexing the matrix $\mathbf{U}$, the index pair (i, j) corresponds to a particular pair of BSs, and thus $u_{i,j} = 0$ unless the BSs are either in the same or two adjacent cells. A similar structure holds for the matrix A. Therefore, both matrices $\mathbf{U}$ and $\mathbf{A}$ will be sparse.

The problem $\mathcal{P}_1$ is a strictly convex problem and strong duality holds. Hence, solving the primal problem is equivalent to solving its corresponding dual problem [4]. More importantly, the dual problem exhibits a decomposable structure, which allows us to decompose the problem into a set of subproblems and solve them in a distributed manner [4]. Specifically, we write down the Lagrangian function:

$$\mathcal{L}(\tilde{\mathbf{x}}, \lambda, \nu) = \tilde{\mathbf{x}}^T\tilde{\mathbf{x}} + \lambda^T(\mathbf{U}\tilde{\mathbf{x}} - \mathbf{b}) + \nu^T(\mathbf{A}\tilde{\mathbf{x}} - \mathbf{c}), \tag{11}$$

where $\lambda \in \mathbb{R}^{4M\times 1} \succeq 0$ and $\nu \in \mathbb{R}^{2M\times 1}$. Note that each dual variable component λ_j or ν_k corresponds to a unique BS m. For a BS m, there is a set of corresponding variables λ_j and ν_k. The dual problem is then defined as

$$\max_{\lambda,\nu} g(\lambda, \nu), \qquad \text{subject to } \lambda \succeq 0, \tag{12}$$

with $g(\lambda, \nu) = \min_{\tilde{\mathbf{x}}} \mathcal{L}(\tilde{\mathbf{x}}, \lambda, \nu)$ being the the dual function. Then one can solve the original problem by finding the optimal dual variables in an iterative manner. Specifically, with the current dual variables $\lambda^{(t)}$ and $\nu^{(t)}$ at the tth iteration, to attain the minimization of Lagrangian, one can set the first-order derivative of the Lagrangian to zero, which leads to

$$\tilde{\mathbf{x}}^{*(t)} = -\frac{1}{2}\left(\mathbf{U}^T\lambda^{(t)} + \mathbf{A}^T\nu^{(t)}\right), \tag{13}$$

or more explicitly,

$$\tilde{x}_n^{*(t)} = -\frac{1}{2}\left(\sum_{j=1}^{4M} u_{j,n}\lambda_j^{(t)} + \sum_{j=1}^{2M} a_{j,n}\nu_j^{(t)}\right), n = 1, \ldots, 2M. \tag{14}$$

Then the dual function is represented as:

$$g(\lambda, \nu) = -\frac{1}{4}\left(\mathbf{U}^T\lambda + \mathbf{A}^T\nu\right)^T\left(\mathbf{U}^T\lambda + \mathbf{A}^T\nu\right) - \lambda^T\mathbf{b} - \nu^T\mathbf{c}.$$

In this way, the dual variables are updated by solving the dual problem of (12) with the new dual function. Instead of using a conventional subgradient method, here we invoke an accelerated gradient method [5] to update the dual variables in order to speed up the convergence of the algorithm. In particular, the dual variables can be updated according to:

$$\begin{aligned} \lambda_j^{(t+1)} &= \Bigg[\lambda_j^{(t)} + \frac{t-1}{t+2}\left(\lambda_j^{(t)} - \lambda_j^{(t-1)}\right) \\ &\quad + \frac{1}{2L}\left(\sum_{l=1}^{2M} u_{j,l}\bar{x}_l^{(t)} - b_j\right)\Bigg]^+, j = 1, \ldots, 4M, \\ \nu_k^{(t+1)} &= \nu_k^{(t)} + \frac{t-1}{t+2}\left(\nu_k^{(t)} - \nu_k^{(t-1)}\right) \\ &\quad + \frac{1}{2L}\left(\sum_{l=1}^{2M} a_{k,l}\bar{x}_l^{(t)} - c_k\right), k = 1, \ldots, 2M, \end{aligned} \tag{15}$$

where $[.]^+$ denotes the projection onto the nonnegative orthant, $L = \left(\|\bar{\mathbf{A}}\bar{\mathbf{A}}^T\|_1\|\bar{\mathbf{A}}\bar{\mathbf{A}}^T\|_\infty\right)^{1/2}$ with $\bar{\mathbf{A}} = [\mathbf{U}^T, \mathbf{A}^T]^T$ and

$$\bar{x}_l^{(t)} = \tilde{x}_l^{*(t)} + \frac{t-1}{t+2}\left(\tilde{x}_l^{*(t)} - \tilde{x}_l^{*(t-1)}\right), l = 1, \ldots, 2M. \tag{16}$$

It is emphasized that to update primal variable $\tilde{x}_n^{*(t)}$ via (14), only dual variables that are associated with BS m and its neighboring BSs are needed due to the sparsity of matrix $\mathbf{U}$ and $\mathbf{A}$. Similarly, to update dual variables $\{\lambda_j^{(t+1)}, \nu_k^{(t+1)}\}$ via (15) at BS m, only primal variables associated with BS m and its neighbors are needed. Also, the step size L can be computed in a distributed fashion [5]. Therefore, local communication between neighboring BSs suffices to find the optimal solution. The distributed algorithm described is summarized in Table II.

V. Simulation Results

In the simulation, the number of BSs $M = 10$; the channels are assumed to be flat fading. The network is symmetric in the sense that: *i)* all the same-cell and inter-cell channels are i.i.d. Rayleigh distributed with variance unity and α^2, respectively; *ii)* symbols required by all MSs are drawn from the same constellation; *iii)* all MSs have the same SEP target.

TABLE II

A DISTRIBUTED ALGORITHM BASED ON PRIMAL-DUAL DECOMPOSITION.

Parameters	L, $\mathbf{U}$, $\mathbf{A}$, $\mathbf{b}$, $\mathbf{c}$;
Initial	set $t = 0$, and dual variables $\lambda^{(0)} > 0$, $\nu^{(0)}$
	Repeat for T iterations:
Step 1.	BS m computes the primal variables $\tilde{x}_n^{*(t)}$ according to (14) for the corresponding $\{n\}$ indices, for $m = 1, \ldots, M$;
Step 2.	BS m shares its primal variables $(\tilde{x}_{2m-1}^{*(t)}, \tilde{x}_{2m}^{*(t)})$ to its adjacent BSs, $m = 1, \ldots, M$;
Step 3.	BS m updates its dual variables $\lambda_j^{(t+1)}$ and $\nu_k^{(t+1)}$ using (15) for the corresponding $\{j, k\}$ indices, for $m = 1, \ldots, M$;
Step 4.	BS m shares the updated dual variables with its neighboring BSs, $m = 1, \ldots, M$.
Step 5.	$t \leftarrow t + 1$ and go to step 1.

Assume that a minimum scaling factor is used for each MS. Given the symmetric setup, scaling factors for the MSs are identical, i.e., $\beta_m = \beta^-$, $\forall m = 1, \ldots, M$. At a specific target, the total power consumption is calculated by averaging over 1000 random realizations, for which random data and channel coefficients are generated. Both 4-QAM and 16-QAM inputs are considered.

Fig. 4 and Fig. 5 plot the transmit power consumption versus the SEP targets for the systems with 4-QAM and 16-QAM signalling, respectively. It is seen that the distributed algorithm is able to attain solutions that converge well to the centralized solutions. This makes the distributed algorithm very attractive since it only requires local communication between BSs.

We also compare the proposed precoding scheme with linear ZF precoding in form of $\mathbf{x}_{\text{ZF}} = \mathbf{H}^T \left(\mathbf{H}\mathbf{H}^T\right)^{-1} (\beta^- \mathbf{d})$. It is shown that the proposed scheme greatly reduces the total power consumption. In particular, the power reduction for the system with 4-QAM is more significant than that for the system with 16-QAM. This is because for the 16-QAM, the power reduction can only be attained when the side and corner constellation points are transmitted. In addition, the exact power reduction from the proposed scheme also depends on the inter-cell gain. As the inter-cell gain decreases, the power reduction decreases as observed from simulation.

VI. CONCLUSIONS

In this work, we have investigated the power-efficient cooperative BS transmission in a distributed network with minimum SEP targets to meet at MSs. A convex-optimization precoding problem is formulated by translating SEP targets into a set of linear constraints. A distributed algorithm has been developed to solve the problem, where local communication between neighboring BSs suffices to produce near-optimal solutions. Numerical results confirm considerable transmit power reduction attained from the proposed scheme, in comparison with the conventional linear ZF precoding.

ACKNOWLEDGEMENT

Supported by the CSIRO Macquarie University Chair in Wireless Communications. This chair has been established with funding provided by the Science and Industry Endowment Fund.

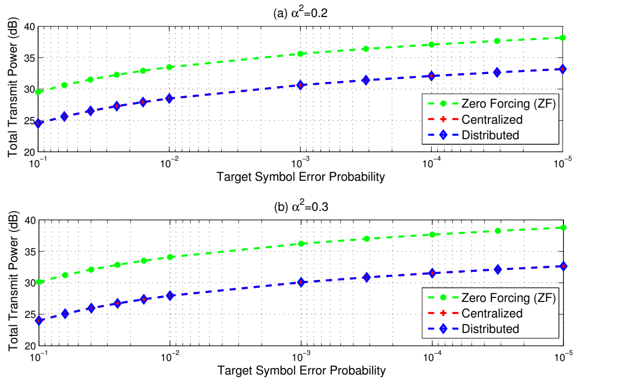

Fig. 4. Total transmit power versus target SEP with 4-QAM inputs: inter-cell gain: (a) $\alpha^2 = 0.2$; (b) $\alpha^2 = 0.3$.

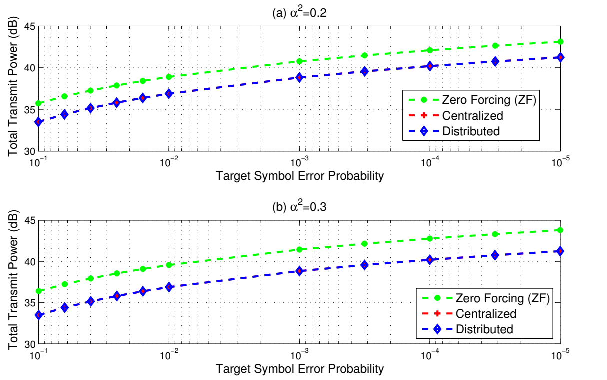

Fig. 5. Total transmit power versus target SEP with 16-QAM inputs: inter-cell gain: (a) $\alpha^2 = 0.2$; (b) $\alpha^2 = 0.3$.

REFERENCES

[1] D. Gesbert, S. Hanly, H. Huang, S. Shamai, O. Simeone, and W. Yu, "Multi-cell MIMO cooperative networks: A new look at interference," *IEEE Journal on Selected Areas in Communications*, vol. 28, no. 9, pp. 1380–1408, 2010.

[2] C. B. Peel, B. M. Hochwald, and A. L. Swindlehurst, "A vector-perturbation technique for near-capacity multiantenna multiuser communication-part I: channel inversion and regularization," *IEEE Transactions on Communications*, vol. 53, no. 1, pp. 195–202, 2005.

[3] R. R. Muller, D. Guo, and A. L. Moustakas, "Vector precoding for wireless MIMO systems and its replica analysis," *IEEE Journal on Selected Areas in Communications*, vol. 26, no. 3, pp. 530–540, 2008.

[4] D. P. Palomar and M. Chiang, "A tutorial on decomposition methods for network utility maximization," *IEEE Journal on Selected Areas in Communications*, vol. 24, no. 8, pp. 1439–1451, 2006.

[5] P. Giselsson, M. D. Doan, T. Keviczky, B. De Schutter, and A. Rantzer, "Accelerated gradient methods and dual decomposition in distributed model predictive control," *Automatica*, vol. 49, no. 3, pp. 828–833, 2013.